Accurate Evaluation of Characteristic Modes

Miloslav Capek[1] Doruk Tayli[2] Lamye Akrou[3] Vit Losenicky[1]
Lukas Jelinek[1] Mats Gustafsson[2]

[1]Department of Electromagnetic Field
Czech Technical University in Prague, Czech Republic
miloslav.capek@fel.cvut.cz

[2]Department of Electrical and Information Technology,
Lund University, Sweden

[3]Department of Electricaland Computer Engineering,
University of Coimbra, Portugal

The 12th European Conference on Antennas and Propagation
London, United Kingdom
April 12, 2018

Outline

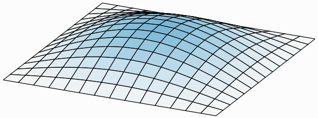

$\boldsymbol{\mathcal{J}}_1(\boldsymbol{r}, t)$

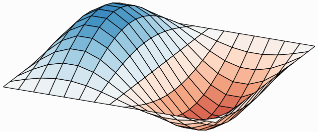

$\boldsymbol{\mathcal{J}}_2(\boldsymbol{r}, t)$

This talk concerns:

- electric currents in vacuum (generalization is, however, straightforward),
- time-harmonic quantities, *i.e.*, $\boldsymbol{\mathcal{A}}(\boldsymbol{r}, t) = \mathrm{Re}\{\boldsymbol{A}(\boldsymbol{r})\exp(\mathrm{j}\omega t)\}$.

Characteristic Mode Decomposition

Generalized eigenvalue problem[1]

$$\mathbf{X}\mathbf{I}_n = \lambda_n \mathbf{R}\mathbf{I}_n,$$

$\mathbf{Z} = \mathbf{R} + \mathrm{j}\mathbf{X} \in \mathbb{C}^{N\times N}$ is impedance matrix, $\mathbf{I}_n \in \mathbb{R}^{N\times 1}$ are expansion coefficients.

[1] R. F. Harrington and J. R. Mautz, "Computation of characteristic modes for conducting bodies", *IEEE Trans. Antennas Propag.*, vol. 19, no. 5, pp. 629–639, 1971. DOI: 10.1109/TAP.1971.1139990

Characteristic Mode Decomposition

Generalized eigenvalue problem[1]

$$\mathbf{X}\mathbf{I}_n = \lambda_n \mathbf{R}\mathbf{I}_n,$$

$\mathbf{Z} = \mathbf{R} + \mathrm{j}\mathbf{X} \in \mathbb{C}^{N\times N}$ is impedance matrix, $\mathbf{I}_n \in \mathbb{R}^{N\times 1}$ are expansion coefficients.

Benefits

- provide physical insight
- formalization of what antenna designers know and understand
- excellent entire-domain basis

[1] R. F. Harrington and J. R. Mautz, "Computation of characteristic modes for conducting bodies", *IEEE Trans. Antennas Propag.*, vol. 19, no. 5, pp. 629–639, 1971. DOI: 10.1109/TAP.1971.1139990

Characteristic Mode Decomposition

Generalized eigenvalue problem[1]

$$\mathbf{X}\mathbf{I}_n = \lambda_n \mathbf{R}\mathbf{I}_n,$$

$\mathbf{Z} = \mathbf{R} + \mathrm{j}\mathbf{X} \in \mathbb{C}^{N\times N}$ is impedance matrix, $\mathbf{I}_n \in \mathbb{R}^{N\times 1}$ are expansion coefficients.

Benefits

- provide physical insight
- formalization of what antenna designers know and understand
- excellent entire-domain basis

but...

- hyped and sometimes misused (since used for everything)
- suffers from numerical problems
- incompatible with realistic feeding

[1] R. F. Harrington and J. R. Mautz, "Computation of characteristic modes for conducting bodies", *IEEE Trans. Antennas Propag.*, vol. 19, no. 5, pp. 629–639, 1971. DOI: 10.1109/TAP.1971.1139990

Characteristic Mode Decomposition

Generalized eigenvalue problem[1]

$$\mathbf{X}\mathbf{I}_n = \lambda_n \mathbf{R}\mathbf{I}_n,$$

$\mathbf{Z} = \mathbf{R} + \mathrm{j}\mathbf{X} \in \mathbb{C}^{N\times N}$ is impedance matrix, $\mathbf{I}_n \in \mathbb{R}^{N\times 1}$ are expansion coefficients.

Benefits

- provide physical insight
- formalization of what antenna designers know and understand
- excellent entire-domain basis

but. . .

- hyped and sometimes misused (since used for everything)
- suffers from numerical problems
- incompatible with realistic feeding

[1] R. F. Harrington and J. R. Mautz, "Computation of characteristic modes for conducting bodies", *IEEE Trans. Antennas Propag.*, vol. 19, no. 5, pp. 629–639, 1971. DOI: 10.1109/TAP.1971.1139990

Benchmark of CM Solvers: Spherical Shell[2], $ka = 1/2$

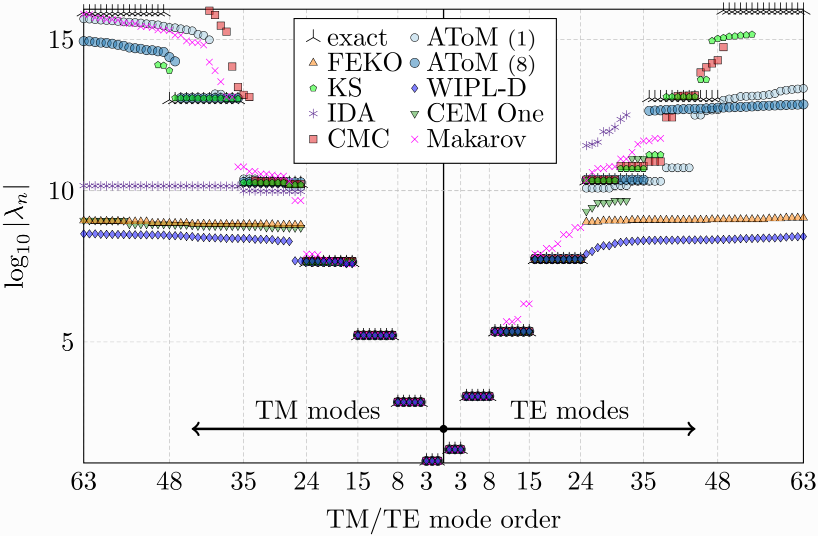

[2] M. Capek, V. Losenicky, L. Jelinek, *et al.*, "Validating the characteristic modes solvers", *IEEE Trans. Antennas Propag.*, vol. 65, no. 8, pp. 4134–4145, 2017. DOI: 10.1109/TAP.2017.2708094

Cause of Limited Number of Modes

Previous benchmark generated some important questions:

- How many modes can, in principle, be found?
- Is there a way how to increase their number?
- Is there a way how to accelerate solution if only few modes are needed?

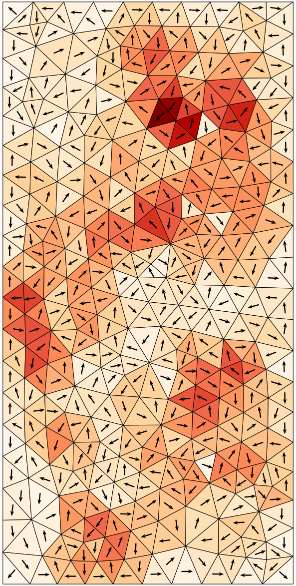

Cause of Limited Number of Modes

Previous benchmark generated some important questions:

- How many modes can, in principle, be found?
- Is there a way how to increase their number?
- Is there a way how to accelerate solution if only few modes are needed?

Problem is predominantly caused by numerical dynamics of the **R** matrix (naive interpretation: only a few modes radiate well. You will see later…).

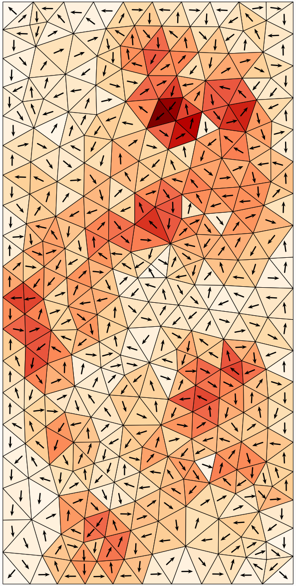

Electric Field Integral Equation (EFIE)

EFIE for PEC bodies as the core of underlying MoM formulation:

$$\hat{\boldsymbol{n}} \times \boldsymbol{E}(\boldsymbol{r}_2) = \mathrm{j} k Z_0 \hat{\boldsymbol{n}} \times \int\limits_{\Omega} \mathbf{G}(\boldsymbol{r}_1, \boldsymbol{r}_2) \cdot \boldsymbol{J}(\boldsymbol{r}_1) \, \mathrm{d}S_1, \tag{1}$$

with dyadic Green function defined as

$$\mathbf{G}(\boldsymbol{r}_1, \boldsymbol{r}_2) = \left(\mathbf{1} + \frac{1}{k^2} \nabla\nabla\right) \frac{\mathrm{e}^{-\mathrm{j}k|\boldsymbol{r}_1 - \boldsymbol{r}_2|}}{4\pi |\boldsymbol{r}_1 - \boldsymbol{r}_2|}. \tag{2}$$

Electric Field Integral Equation (EFIE)

EFIE for PEC bodies as the core of underlying MoM formulation:

$$\hat{\boldsymbol{n}} \times \boldsymbol{E}(\boldsymbol{r}_2) = \mathrm{j}kZ_0 \hat{\boldsymbol{n}} \times \int\limits_{\Omega} \mathbf{G}(\boldsymbol{r}_1, \boldsymbol{r}_2) \cdot \boldsymbol{J}(\boldsymbol{r}_1) \, \mathrm{d}S_1, \tag{1}$$

with dyadic Green function defined as

$$\mathbf{G}(\boldsymbol{r}_1, \boldsymbol{r}_2) = \left(\mathbf{1} + \frac{1}{k^2}\nabla\nabla\right) \frac{\mathrm{e}^{-\mathrm{j}k|\boldsymbol{r}_1 - \boldsymbol{r}_2|}}{4\pi |\boldsymbol{r}_1 - \boldsymbol{r}_2|}. \tag{2}$$

The impedance matrix **Z** reads

$$Z_{pq} = \mathrm{j}kZ_0 \int\limits_{\Omega} \int\limits_{\Omega} \boldsymbol{\psi}_p(\boldsymbol{r}_1) \cdot \mathbf{G}(\boldsymbol{r}_1, \boldsymbol{r}_2) \cdot \boldsymbol{\psi}_q(\boldsymbol{r}_2) \, \mathrm{d}S_1 \, \mathrm{d}S_2. \tag{3}$$

Spherical Wave Expansion of Dyadic Green Function

Spherical wave expansion of dyadic Green function reads[3]

$$\mathbf{G}\left(\boldsymbol{r}_1, \boldsymbol{r}_2\right) = -\mathrm{j}k \sum_{\alpha} \mathbf{u}_{\alpha}^{(1)}\left(k\boldsymbol{r}_<\right) \mathbf{u}_{\alpha}^{(4)}\left(k\boldsymbol{r}_>\right). \tag{4}$$

[3] G. Kristensson, *Scattering of electromagnetic waves by obstacles*. Edison, NJ: SciTech Publishing, an imprint of the IET, 2016

Spherical Wave Expansion of Dyadic Green Function

Spherical wave expansion of dyadic Green function reads[3]

$$\mathbf{G}\left(\boldsymbol{r}_1, \boldsymbol{r}_2\right) = -\mathrm{j}k \sum_{\alpha} \mathbf{u}_{\alpha}^{(1)}\left(k\boldsymbol{r}_<\right) \mathbf{u}_{\alpha}^{(4)}\left(k\boldsymbol{r}_>\right). \tag{4}$$

Impedance matrix $\mathbf{Z}$ with spherical wave expansion substituted

$$Z_{pq} = k^2 Z_0 \sum_{\alpha} \int_{\Omega} \int_{\Omega} \boldsymbol{\psi}_p\left(\boldsymbol{r}_1\right) \cdot \mathbf{u}_{\alpha}^{(1)}\left(k\boldsymbol{r}_<\right) \mathbf{u}_{\alpha}^{(4)}\left(k\boldsymbol{r}_>\right) \cdot \boldsymbol{\psi}_q\left(\boldsymbol{r}_2\right) \mathrm{d}S_1 \, \mathrm{d}S_2. \tag{5}$$

[3] G. Kristensson, *Scattering of electromagnetic waves by obstacles*. Edison, NJ: SciTech Publishing, an imprint of the IET, 2016

Spherical Wave Expansion of Dyadic Green Function

Spherical wave expansion of dyadic Green function reads[3]

$$\mathbf{G}\left(\boldsymbol{r}_1, \boldsymbol{r}_2\right) = -\mathrm{j}k \sum_{\alpha} \mathbf{u}_{\alpha}^{(1)}\left(k\boldsymbol{r}_<\right) \mathbf{u}_{\alpha}^{(4)}\left(k\boldsymbol{r}_>\right). \tag{4}$$

Impedance matrix **Z** with spherical wave expansion substituted

$$Z_{pq} = k^2 Z_0 \sum_{\alpha} \int_{\Omega} \int_{\Omega} \boldsymbol{\psi}_p\left(\boldsymbol{r}_1\right) \cdot \mathbf{u}_{\alpha}^{(1)}\left(k\boldsymbol{r}_<\right) \mathbf{u}_{\alpha}^{(4)}\left(k\boldsymbol{r}_>\right) \cdot \boldsymbol{\psi}_q\left(\boldsymbol{r}_2\right) \mathrm{d}S_1 \, \mathrm{d}S_2. \tag{5}$$

can be used for reformulation of matrix **R** since $\mathbf{u}_{\alpha}^{(1)}\left(k\boldsymbol{r}\right) = \mathrm{Re}\{\mathbf{u}_{\alpha}^{(4)}\left(k\boldsymbol{r}\right)\}$ as

$$R_{pq} = k^2 Z_0 \sum_{\alpha} \int_{\Omega} \boldsymbol{\psi}_p\left(\boldsymbol{r}_1\right) \cdot \mathbf{u}_{\alpha}^{(1)}\left(k\boldsymbol{r}_1\right) \mathrm{d}S_1 \int_{\Omega} \mathbf{u}_{\alpha}^{(1)}\left(k\boldsymbol{r}_2\right) \cdot \boldsymbol{\psi}_q\left(\boldsymbol{r}_2\right) \mathrm{d}S_2 \tag{6}$$

[3] G. Kristensson, *Scattering of electromagnetic waves by obstacles*. Edison, NJ: SciTech Publishing, an imprint of the IET, 2016

Spherical Wave Expansion of Dyadic Green Function

Spherical wave expansion of dyadic Green function reads[3]

$$\mathbf{G}\left(\boldsymbol{r}_1, \boldsymbol{r}_2\right) = -\mathrm{j}k \sum_{\alpha} \mathbf{u}_{\alpha}^{(1)}\left(k\boldsymbol{r}_<\right) \mathbf{u}_{\alpha}^{(4)}\left(k\boldsymbol{r}_>\right). \tag{4}$$

Impedance matrix **Z** with spherical wave expansion substituted

$$Z_{pq} = k^2 Z_0 \sum_{\alpha} \int_{\Omega} \int_{\Omega} \boldsymbol{\psi}_p\left(\boldsymbol{r}_1\right) \cdot \mathbf{u}_{\alpha}^{(1)}\left(k\boldsymbol{r}_<\right) \mathbf{u}_{\alpha}^{(4)}\left(k\boldsymbol{r}_>\right) \cdot \boldsymbol{\psi}_q\left(\boldsymbol{r}_2\right) \mathrm{d}S_1 \, \mathrm{d}S_2. \tag{5}$$

can be used for reformulation of matrix **R** since $\mathbf{u}_{\alpha}^{(1)}\left(k\boldsymbol{r}\right) = \mathrm{Re}\{\mathbf{u}_{\alpha}^{(4)}\left(k\boldsymbol{r}\right)\}$ as

$$R_{pq} = k^2 Z_0 \sum_{\alpha} \left(\int_{\Omega} \boldsymbol{\psi}_p\left(\boldsymbol{r}_1\right) \cdot \mathbf{u}_{\alpha}^{(1)}\left(k\boldsymbol{r}_1\right) \mathrm{d}S_1\right) \left(\int_{\Omega} \mathbf{u}_{\alpha}^{(1)}\left(k\boldsymbol{r}_2\right) \cdot \boldsymbol{\psi}_q\left(\boldsymbol{r}_2\right) \mathrm{d}S_2\right)$$

[3] G. Kristensson, *Scattering of electromagnetic waves by obstacles*. Edison, NJ: SciTech Publishing, an imprint of the IET, 2016

Definition of Projection Matrix **S**

Resistance matrix **R** is expressed as a product of two identical rectangular matrices:

$$R_{pq} = \sum_{\alpha} \left(k\sqrt{Z_0} \int_{\Omega} \boldsymbol{\psi}_p \left(\boldsymbol{r}_1\right) \cdot \mathbf{u}_{\alpha}^{(1)} \left(k\boldsymbol{r}_1\right) \, \mathrm{d}S_1 \right) \left(k\sqrt{Z_0} \int_{\Omega} \mathbf{u}_{\alpha}^{(1)} \left(k\boldsymbol{r}_2\right) \cdot \boldsymbol{\psi}_q \left(\boldsymbol{r}_2\right) \, \mathrm{d}S_2 \right)$$

Definition of Projection Matrix **S**

Resistance matrix $\mathbf{R}$ is expressed as a product of two identical rectangular matrices:

$$R_{pq} = \sum_{\alpha} \left(k\sqrt{Z_0} \int_{\Omega} \boldsymbol{\psi}_p \left(\boldsymbol{r}_1\right) \cdot \mathbf{u}_{\alpha}^{(1)} \left(k\boldsymbol{r}_1\right) \, \mathrm{d}S_1 \right) \left(k\sqrt{Z_0} \int_{\Omega} \mathbf{u}_{\alpha}^{(1)} \left(k\boldsymbol{r}_2\right) \cdot \boldsymbol{\psi}_q \left(\boldsymbol{r}_2\right) \, \mathrm{d}S_2 \right)$$

Definition[4] of the matrix $\mathbf{S} \in \mathbb{R}^{N_\alpha \times N}$

$$S_{\alpha p} = k\sqrt{Z_0} \int_{\Omega} \boldsymbol{\psi}_p \left(\boldsymbol{r}\right) \cdot \mathbf{u}_{\alpha}^{(1)} \left(k\boldsymbol{r}\right) \, \mathrm{d}S, \tag{6}$$

and its relation to the resistance matrix

$$\mathbf{R} = \mathbf{S}^{\mathrm{T}}\mathbf{S}. \tag{7}$$

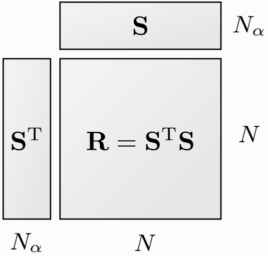

[4] D. Tayli, M. Capek, L. Akrou, *et al.*, "Accurate and efficient evaluation of characteristic modes", , 2017, submitted, arXiv:1709.09976. [Online]. Available: https://arxiv.org/abs/1709.09976

Properties of Matrix **S**, Part #1

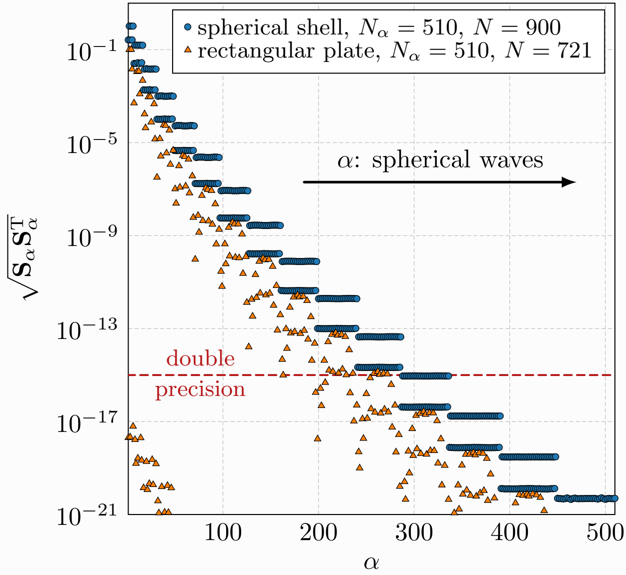

Properties of Matrix **S**, Part #1

- Matrix **S** is real-valued, rectangular, low-rank

$$N_\alpha = 2L\left(L+2\right), \tag{8}$$

$$L = \lceil ka + 7\sqrt[3]{ka} + 2 \rceil. \tag{9}$$

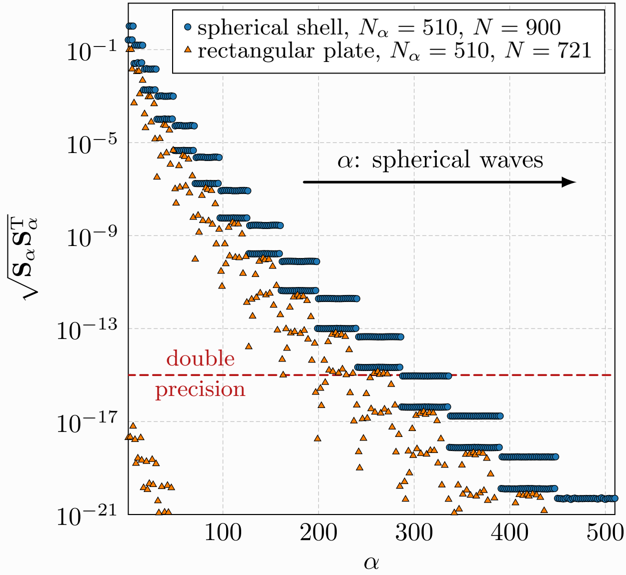

Properties of Matrix **S**, Part #1

- Matrix **S** is real-valued, rectangular, low-rank

$$N_\alpha = 2L\left(L+2\right), \quad (8)$$

$$L = \left\lceil ka + 7\sqrt[3]{ka} + 2 \right\rceil. \quad (9)$$

- Matrix $\mathbf{S}^{\mathrm{T}}\mathbf{S}$ does not contain any negative eigenvalue higher than numerical noise.

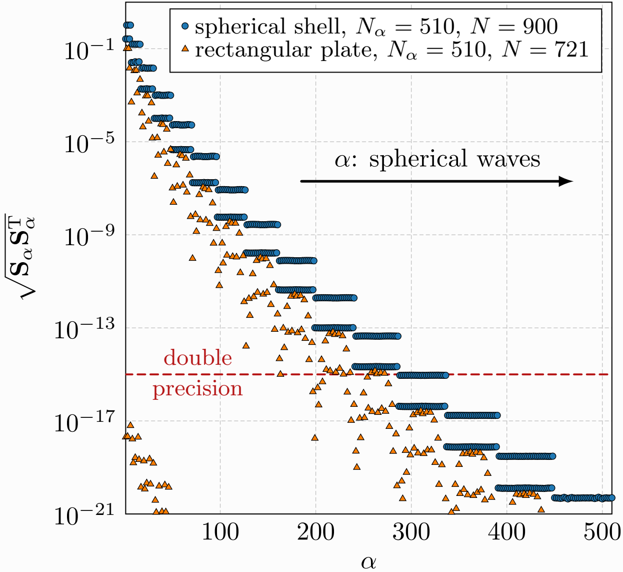

Properties of Matrix **S**, Part #1

- Matrix **S** is real-valued, rectangular, low-rank

$$N_\alpha = 2L\left(L+2\right), \qquad (8)$$

$$L = \left\lceil ka + 7\sqrt[3]{ka} + 2 \right\rceil. \qquad (9)$$

- Matrix $\mathbf{S}^{\mathrm{T}}\mathbf{S}$ does not contain any negative eigenvalue higher than numerical noise.
- Matrix **S** represents projection between RWGs and spherical waves, *i.e.*,

$$\mathbf{R} = \mathbf{S}^{\mathrm{T}}\mathbf{S}, \qquad (10)$$

$$\mathbf{R}^{\mathrm{sph}} = \mathbf{S}\mathbf{S}^{\mathrm{T}}. \qquad (11)$$

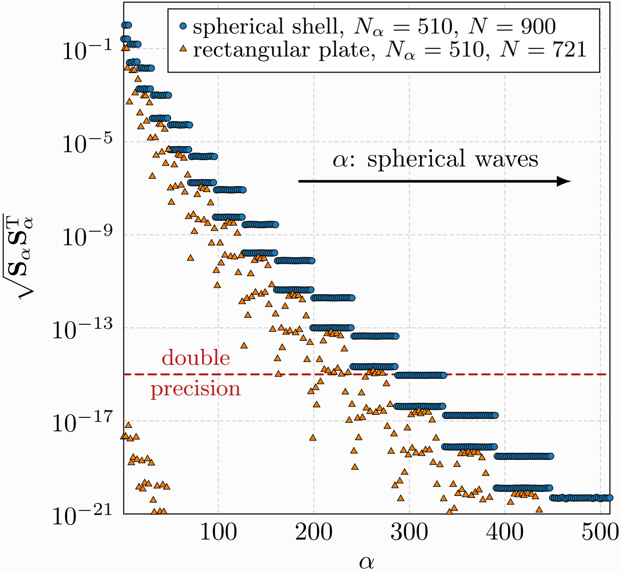

Properties of Matrix **S**, Part #2

Radiated power can be calculated as

$$P_{\mathrm{rad}} = \frac{1}{2Z_0} \int\limits_{S^2} \left| \boldsymbol{F}\left(\hat{\boldsymbol{r}}\right) \right|^2 \, \mathrm{d}S \approx \frac{1}{2} \mathbf{I}^{\mathrm{H}} \mathbf{R} \mathbf{I} = \frac{1}{2} \left| \mathbf{S} \mathbf{I} \right|^2 = \frac{1}{2} \sum_{\alpha} \left| f_\alpha \right|^2 \tag{12}$$

with

$$\boldsymbol{F}\left(\hat{\boldsymbol{r}}\right) = \frac{1}{k} \sum_{\alpha} \mathrm{j}^{l-\tau+2} f_\alpha \mathbf{Y}_\alpha \left(\hat{\boldsymbol{r}}\right), \tag{13}$$

where $\mathbf{Y}_\alpha \left(\hat{\boldsymbol{r}}\right)$ are the real-valued spherical vector harmonics.

Properties of Matrix S, Part #2

Radiated power can be calculated as

$$P_{\mathrm{rad}} = \frac{1}{2Z_0} \int\limits_{S^2} \left|\boldsymbol{F}\left(\hat{\boldsymbol{r}}\right)\right|^2 \mathrm{d}S \approx \frac{1}{2}\mathbf{I}^{\mathrm{H}}\mathbf{R}\mathbf{I} = \frac{1}{2}\left|\mathbf{S}\mathbf{I}\right|^2 = \frac{1}{2}\sum_{\alpha}\left|f_\alpha\right|^2 \tag{12}$$

with

$$\boldsymbol{F}\left(\hat{\boldsymbol{r}}\right) = \frac{1}{k}\sum_{\alpha} \mathrm{j}^{l-\tau+2} f_\alpha \mathbf{Y}_\alpha\left(\hat{\boldsymbol{r}}\right), \tag{13}$$

where $\mathbf{Y}_\alpha\left(\hat{\boldsymbol{r}}\right)$ are the real-valued spherical vector harmonics.

Example			Comp. times in IDA (s)		
	N_α	N	$\mathbf{R}$	$\mathbf{S}$	$\mathbf{R} = \mathbf{S}^{\mathrm{T}}\mathbf{S}$
spherical shell	880	750	0.09	0.009	0.011
spherical shell	880	3330	1.78	0.039	0.083
helicopter	880	18898	54.50	0.236	1.660

CMs Using SVD of matrix $\mathbf{S}$ and GEP Partitioning

Singular value decomposition (SVD) of matrix $\mathbf{S}$

$$\mathbf{S} = \mathbf{U}\mathbf{\Lambda}\mathbf{V}^{\mathrm{H}}, \tag{14}$$

substituted into CM definition gives

$$\left(\mathbf{V}^{\mathrm{H}}\mathbf{X}\mathbf{V}\right)\left(\mathbf{V}^{\mathrm{H}}\mathbf{I}_n\right) = \lambda_n \left(\mathbf{\Lambda}^{\mathrm{H}}\mathbf{\Lambda}\right)\left(\mathbf{V}^{\mathrm{H}}\mathbf{I}_n\right) \quad \longrightarrow \quad \widetilde{\mathbf{X}}\widetilde{\mathbf{I}}_n = \lambda_n \widetilde{\mathbf{R}}\widetilde{\mathbf{I}}_n, \tag{15}$$

CMs Using SVD of matrix $\mathbf{S}$ and GEP Partitioning

Singular value decomposition (SVD) of matrix $\mathbf{S}$

$$\mathbf{S} = \mathbf{U}\mathbf{\Lambda}\mathbf{V}^{\mathrm{H}}, \tag{14}$$

substituted into CM definition gives

$$\left(\mathbf{V}^{\mathrm{H}}\mathbf{X}\mathbf{V}\right)\left(\mathbf{V}^{\mathrm{H}}\mathbf{I}_n\right) = \lambda_n \left(\mathbf{\Lambda}^{\mathrm{H}}\mathbf{\Lambda}\right)\left(\mathbf{V}^{\mathrm{H}}\mathbf{I}_n\right) \quad \longrightarrow \quad \widetilde{\mathbf{X}}\widetilde{\mathbf{I}}_n = \lambda_n \widetilde{\mathbf{R}}\widetilde{\mathbf{I}}_n, \tag{15}$$

Partitioning

$$\widetilde{\mathbf{X}}\widetilde{\mathbf{I}} = \begin{pmatrix} \widetilde{\mathbf{X}}_{11} & \widetilde{\mathbf{X}}_{12} \\ \widetilde{\mathbf{X}}_{21} & \widetilde{\mathbf{X}}_{22} \end{pmatrix} \begin{pmatrix} \widetilde{\mathbf{I}}_{1n} \\ \widetilde{\mathbf{I}}_{2n} \end{pmatrix} = \begin{pmatrix} \lambda_{1n} \widetilde{\mathbf{R}}_{11} \widetilde{\mathbf{I}}_{1n} \\ \mathbf{0} \end{pmatrix} \tag{16}$$

and reducing to Schur complement yields the final GEP formulation

$$\left(\widetilde{\mathbf{X}}_{11} - \widetilde{\mathbf{X}}_{12}\widetilde{\mathbf{X}}_{22}^{-1}\widetilde{\mathbf{X}}_{21}\right)\widetilde{\mathbf{I}}_{1n} = \lambda_{1n}\widetilde{\mathbf{R}}_{11}\widetilde{\mathbf{I}}_{1n}. \tag{17}$$

Properties of the Decomposition:

Characteristic modes are constructed as

$$\widetilde{\mathbf{I}}_n = \begin{pmatrix} \widetilde{\mathbf{I}}_{1n} \\ -\widetilde{\mathbf{X}}_{22}^{-1}\widetilde{\mathbf{X}}_{21}\widetilde{\mathbf{I}}_{1n} \end{pmatrix}, \tag{18}$$

radiated power is implicitly normalized by $\mathbf{\Lambda}^{\mathrm{H}}\mathbf{\Lambda}$ matrix in (15)

$$\widetilde{\mathbf{I}}_n^{\mathrm{H}}\widetilde{\mathbf{R}}\widetilde{\mathbf{I}}_m = \delta_{nm}. \tag{19}$$

[4] D. Tayli, M. Capek, L. Akrou, *et al.*, "Accurate and efficient evaluation of characteristic modes", , 2017, submitted, arXiv:1709.09976. [Online]. Available: https://arxiv.org/abs/1709.09976

Properties of the Decomposition:

Characteristic modes are constructed as

$$\widetilde{\mathbf{I}}_n = \begin{pmatrix} \widetilde{\mathbf{I}}_{1n} \\ -\widetilde{\mathbf{X}}_{22}^{-1}\widetilde{\mathbf{X}}_{21}\widetilde{\mathbf{I}}_{1n} \end{pmatrix}, \tag{18}$$

radiated power is implicitly normalized by $\mathbf{\Lambda}^{\mathrm{H}}\mathbf{\Lambda}$ matrix in (15)

$$\widetilde{\mathbf{I}}_n^{\mathrm{H}}\widetilde{\mathbf{R}}\widetilde{\mathbf{I}}_m = \delta_{nm}. \tag{19}$$

Properties[4]:

- numerical dynamics doubled thanks to the SVD and partitioning,
- number of used spherical modes controls the number of CMs,
- for $N_\alpha \ll N$ (always fulfilled in ESA regime) remarkable speed-up.

[4] D. Tayli, M. Capek, L. Akrou, *et al.*, “Accurate and efficient evaluation of characteristic modes”, , 2017, submitted, arXiv:1709.09976. [Online]. Available: https://arxiv.org/abs/1709.09976

Spherical Shell

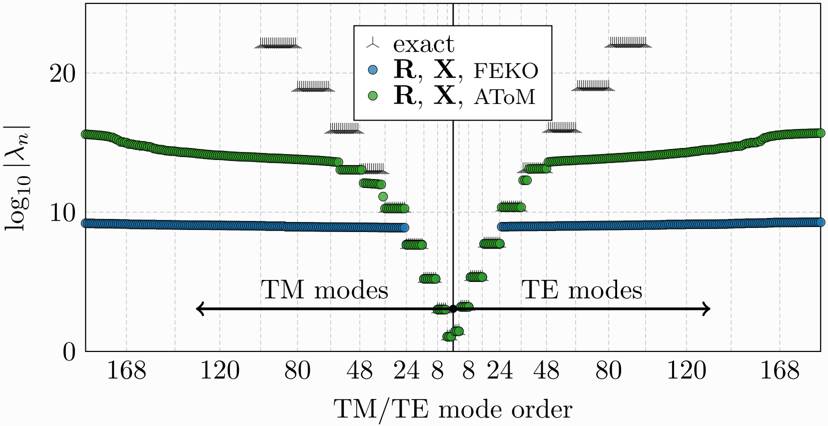

Spherical Shell

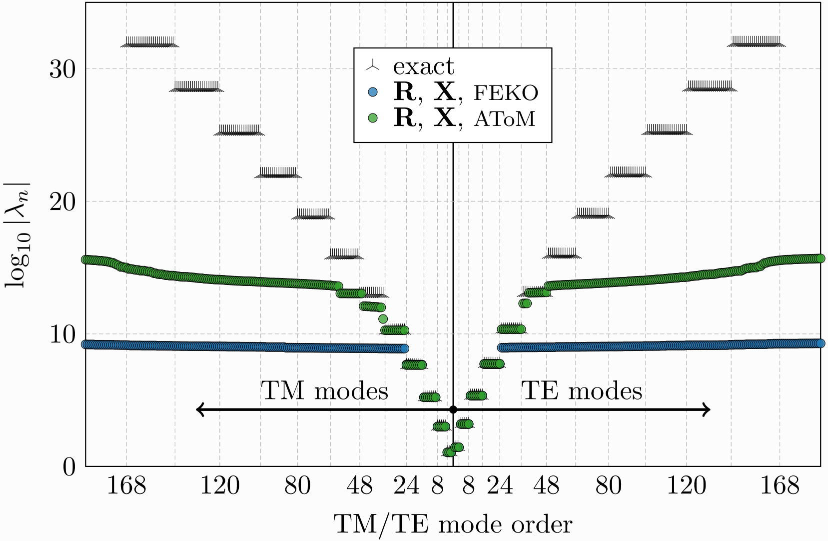

Spherical Shell

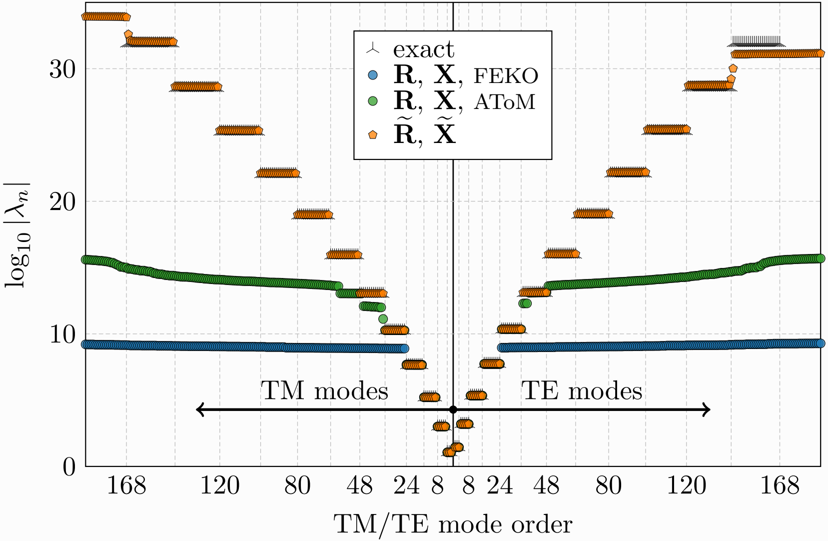

Rectangular Plate

100 modes were calculated (`eigs`)

- $(\mathbf{X}, \mathbf{R})$ 0.7 s (29)
- $(\mathbf{X}, \mathbf{R})$ + Advanpix: 1324 s
- $(\widetilde{\mathbf{X}}, \widetilde{\mathbf{R}})$ 0.5 s (37)

(If matrix $\mathbf{S}$ is reduced, calculation further accelerated.)

Rectangular Plate

100 modes were calculated (`eigs`)

- $(\mathbf{X}, \mathbf{R})$ 0.7 s (29)
- $(\mathbf{X}, \mathbf{R})$ + Advanpix: 1324 s
- $(\widetilde{\mathbf{X}}, \widetilde{\mathbf{R}})$ 0.5 s (37)

(If matrix **S** is reduced, calculation further accelerated.)

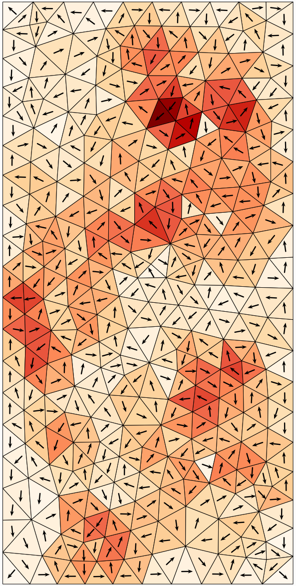

Rectangular Plate

100 modes were calculated (`eigs`)

- ($\mathbf{X}$, $\mathbf{R}$) 0.7 s (29)
- ($\mathbf{X}$, $\mathbf{R}$) + Advanpix: 1324 s
- ($\widetilde{\mathbf{X}}$, $\widetilde{\mathbf{R}}$) 0.5 s (37)

(If matrix **S** is reduced, calculation further accelerated.)

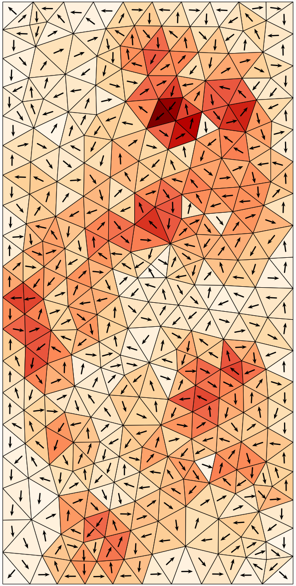

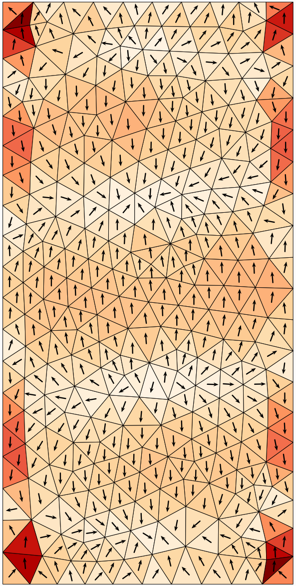

Rectangular Plate – Higher-order Modes

Two high-order modes of rectangular plate:

- left: inductive, $n = 17$, $\lambda_{17} = 2.461 \cdot 10^{17}$,
- right: capacitive, $n = 77$, $\lambda_{77} = -1.947 \cdot 10^{24}$.

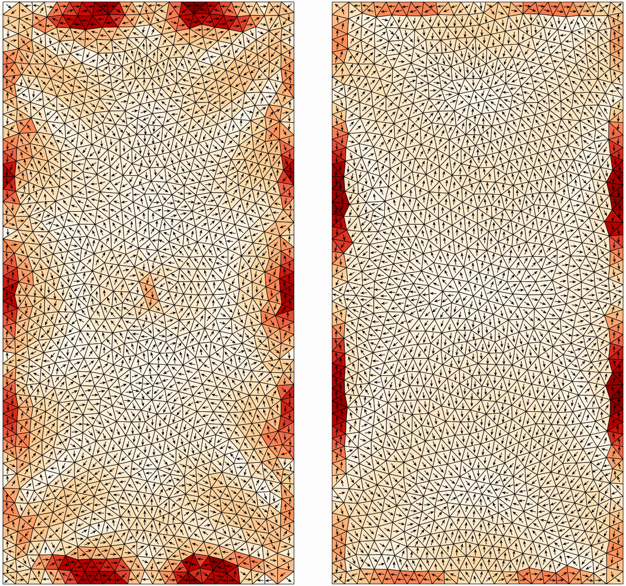

Rectangular Plate – Higher-order Modes

Two high-order modes of rectangular plate:

- left: inductive, $n = 17$, $\lambda_{17} = 2.461 \cdot 10^{17}$,
- right: capacitive, $n = 77$, $\lambda_{77} = -1.947 \cdot 10^{24}$.

Such high-order modes are not needed in practice (except tracking).

- However, accuracy can be interchanged for comp. speed.

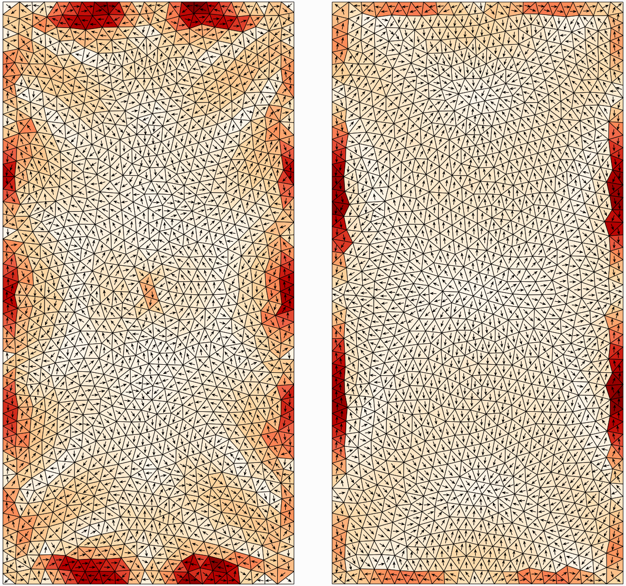

Acceleration of the CMs Decomposition

If double precision is enough, however, computational speed is required:

$$\mathbf{X}\mathbf{I}_n = \lambda_n \mathbf{S}^{\mathrm{T}} \mathbf{S} \mathbf{I}_n \tag{20}$$

Acceleration of the CMs Decomposition

If double precision is enough, however, computational speed is required:

$$\mathbf{X}\mathbf{I}_n = \lambda_n \mathbf{S}^{\mathrm{T}} \mathbf{S} \mathbf{I}_n \tag{20}$$

$$\mathbf{S}\mathbf{I}_n = \lambda_n \mathbf{S}\mathbf{X}^{-1} \mathbf{S}^{\mathrm{T}} \mathbf{S} \mathbf{I}_n \quad \longrightarrow \quad \widehat{\mathbf{X}}\widehat{\mathbf{I}}_n = \xi_n \widehat{\mathbf{I}}_n \tag{21}$$

with $\widehat{\mathbf{X}} = \mathbf{S}\mathbf{X}^{-1}\mathbf{S}^{\mathrm{T}}$, $\widehat{\mathbf{I}}_n = \mathbf{S}\mathbf{I}$, and $\xi_n = 1/\lambda_n$.

Acceleration of the CMs Decomposition

If double precision is enough, however, computational speed is required:

$$\mathbf{X}\mathbf{I}_n = \lambda_n \mathbf{S}^{\mathrm{T}} \mathbf{S} \mathbf{I}_n \tag{20}$$

$$\mathbf{S}\mathbf{I}_n = \lambda_n \mathbf{S}\mathbf{X}^{-1}\mathbf{S}^{\mathrm{T}} \mathbf{S} \mathbf{I}_n \quad \longrightarrow \quad \widehat{\mathbf{X}}\widehat{\mathbf{I}}_n = \xi_n \widehat{\mathbf{I}}_n \tag{21}$$

with $\widehat{\mathbf{X}} = \mathbf{S}\mathbf{X}^{-1}\mathbf{S}^{\mathrm{T}}$, $\widehat{\mathbf{I}}_n = \mathbf{S}\mathbf{I}$, and $\xi_n = 1/\lambda_n$.

Properties:

- solved in basis of spherical waves ($\widehat{\mathbf{I}}_n = \mathbf{S}\mathbf{I}$),
- standard (not generalized) eigenvalue problem,
- solution of typically small $N_\alpha \times N_\alpha$ eigenvalue problem (extreme speed-up),
- all modes, well-represented in the spherical basis, are found,
- `eig` shall be used instead of `eigs` in MATLAB.

Acceleration of the CMs Decomposition – Comparison

Example				Comp. times (s)		
	CMs	N_α	N	$(\mathbf{R}, \mathbf{X})$	$(\widetilde{\mathbf{R}}, \widetilde{\mathbf{X}})$	$(\mathbf{S}\mathbf{X}^{-1}\mathbf{S}^{\mathrm{T}})$
rectangular plate	100	510	655	0.7	0.8	0.5 (510 modes)
spherical shell	300	880	3330	**29**	6.7	**2.6** (880 modes)
helicopter	25	880	18898	**149**	170	**47** (880 modes)
helicopter	100	880	18898	**473**	173	**47** (880 modes)

Windows Server 2012, 2×XEON E5-2665 @ 2.4 GHZ, 72 GB RAM

Acceleration of the CMs Decomposition – Comparison

Example	CMs	N_α	N	Comp. times (s) $(\mathbf{R}, \mathbf{X})$	$(\widetilde{\mathbf{R}}, \widetilde{\mathbf{X}})$	$(\mathbf{S}\mathbf{X}^{-1}\mathbf{S}^{\mathrm{T}})$	
rectangular plate	100	510	655	0.7	0.8	0.5	(510 modes)
spherical shell	300	880	3330	**29**	6.7	**2.6**	(880 modes)
helicopter	25	880	18898	**149**	170	**47**	(880 modes)
helicopter	100	880	18898	**473**	173	**47**	(880 modes)

Windows Server 2012, 2×XEON E5-2665 @ 2.4 GHZ, 72 GB RAM

- $(\widetilde{\mathbf{R}}, \widetilde{\mathbf{X}})$ gives *significantly more* modes accurately and is *typically faster*.
- $(\mathbf{S}\mathbf{X}^{-1}\mathbf{S}^{\mathrm{T}})$ gives *slightly more* modes accurately and is *significantly faster*.
- $(\mathbf{S}\mathbf{X}^{-1}\mathbf{S}^{\mathrm{T}})$ finds all modes available from a given set of spherical harmonics.
- $(\mathbf{S}\mathbf{X}^{-1}\mathbf{S}^{\mathrm{T}})$ decomposition is excellent for high ka with large DOFs N.

Restriction to TM/TE Modes

Matrix $\mathbf{S}^{\mathrm{TM/TE}} = \mathbf{S}\left(i,:\right)$ contains TE and TM modes in separate rows.

Restriction to TM/TE Modes

Matrix $\mathbf{S}^{\mathrm{TM/TE}} = \mathbf{S}(i,:)$ contains TE and TM modes in separate rows.

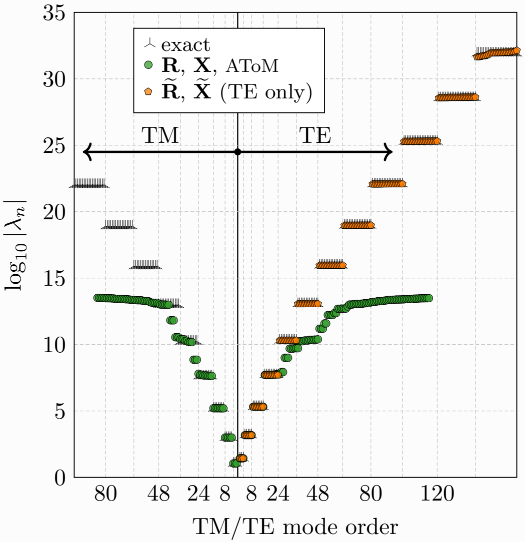

Restriction to TM/TE Modes

Matrix $\mathbf{S}^{\mathrm{TM/TE}} = \mathbf{S}(i,:)$ contains TE and TM modes in separate rows.

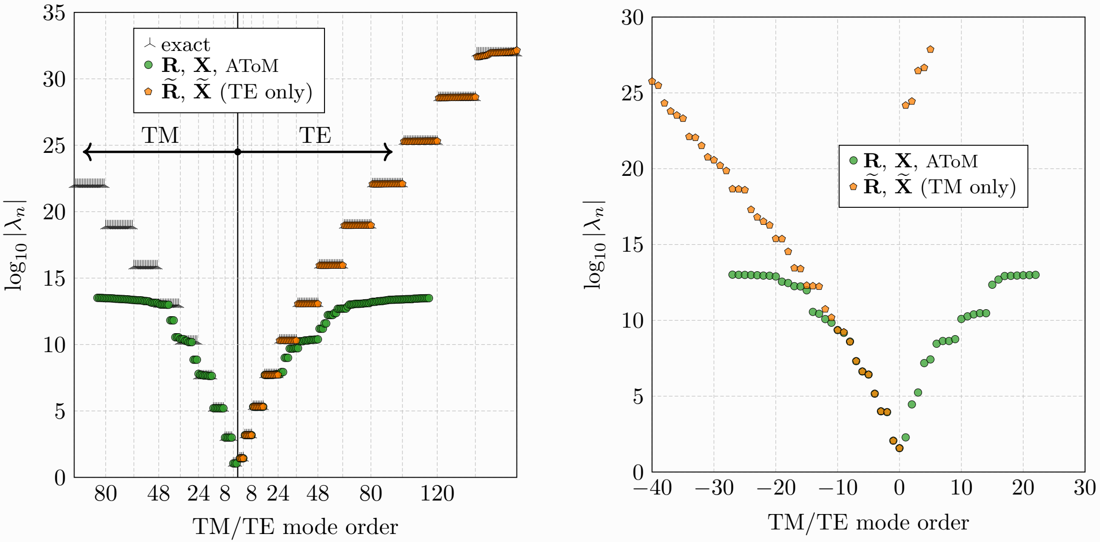

Conclusions

- New matrix operator based on MoM formalism,
- matrix $\mathbf{S}$ has controllable and predictable behavior and numerically neat properties,
- matrix $\mathbf{S}$ has many applications (some of them probably yet unknown),
- if $\mathbf{X}$ is not needed, matrix $\mathbf{S}$ should be preferred over $\mathbf{R}$,
- with respect to the (characteristic) modes, the matrix $\mathbf{S}$ is, in certain sense, a return to their scattering origin[5].

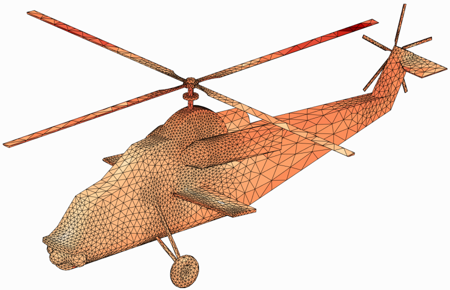

Dominant characteristic mode of helicopter model discretized into 18989 RWGs, $ka = 1/2$.

[5] C. G. Montgomery, R. H. Dicke, and E. M. Purcell, *Principles of microwave circuits*. New York, United States: McGraw-Hill, 1948
R. J. Garbacz, "A generalized expansion for radiated and scattered fields", PhD thesis, Department of Electrical Engineering, Ohio State University, 1968

Questions?

For a complete PDF presentation see ▸ capek.elmag.org

Miloslav Čapek
miloslav.capek@fel.cvut.cz

12. 04. 2018, v1.0